## Quantification of epithelial volume by image processing applied to ovarian tumors

Schipper, N.W.; Smeulders, A.W.M.; Baak, J.P.A.

# Quantification of Epithelial Volume by Image Processing Applied to Ovarian Tumors[1]

## N.W. Schipper, A.W.M. Smeulders, and J.P.A. Baak

Pattern Recognition Group, Department of Applied Physics, Delft University of Technology, Delft (N.W.S.), and Departments of Medical Informatics (A.W.M.S.) and Pathology (J.P.A.B.), Free University, Amsterdam, The Netherlands

This paper describes an image analysis technique for automated estimation of the percentages of epithelium and stroma in (tumor) tissue. The program is evaluated on ovarian tumors of the serous, mucinous, and endometrioid type. From standard paraffin sections, stained with pararosanilin Feulgen and naphthol yellow, a blue-yellow image pair was recorded. The blue image was used for the determination of the total tissue area and the yellow image for the epithelial area. For the latter the image processing method is based on the fact that epithelial nuclei are generally more tightly packed than stromal nuclei. A structural approach was applied, in which the segmentation of the nuclei was based on the image contrast range in the density domain. The method has been tested with 78 image pairs from 19 ovarian tumors with varying degrees of malignancy. The area percentages, as assessed with image processing, were strongly correlated to control percentages, established by interactive morphometry (r = 0.98).

Key terms: Image analysis, ovary, tissue section, epithelial percentage.

In general the survival of patients with ovarian carcinomas is poor. The overall 5-year survival is 30% for carcinomas (16), but varies dependent on stage and grade (15). Subjective grading methods allow the distinction of subsets within the ovarian epithelial tumors (borderline, well differentiated, and moderately to poorly differentiated) with a completely different prognosis.

Although such grades are important prognostic factors (5), their assignment is subjective and not highly reproducible. Within the same grade, as determined by different pathologists, a considerable diagnostic variability can occur. For the ovarian tumors this disagreement between different pathologists has been reported to be as high as 25% (3,10).

Quantitative techniques are urged, to prevent undesired consequences of falsely positive and falsely negative diagnoses and to improve the reproducibility and consistency of the assessment of survival probability. Objective criteria that describe cell and tissue characteristics of (ovarian) tumors are, among others, the cellular DNA content (1,8) and mitotic activity (5,12).

An important histological characteristic of ovarian tumors is the volume percentage of epithelium. In one study (2), this histological feature is one of five features that gave the best discrimination between borderline and malignant ovarian tumors. The feature has been shown to aid prediction of the outcome of patients with borderline tumors and invasive carcinomas (4).

The volume percentage of epithelium in the organ is estimated through measurement of the area percentage of epithelium in tissue slides. The epithelial area can be estimated through interactive morphometry. Practical application in diagnostic pathology, however, requires accurate counting of points, and is a tedious and time-consuming task. A considerable number of microscopic tissue fields is required to reach sufficient accuracy and although the counting procedure is reproducible, the selection of microscopic fields may introduce undesired subjectivity. Therefore digital image processing was explored as a means of estimating the area of epithelium automatically.

In this image processing study the major focus is on segmenting the image into an epithelium part and a stroma part. Afterwards, simply adding the pixels in both parts suffices to arrive at the desired epithelium:tissue ratio. Several factors complicate this seg-

mentation. The algorithm should be resistant against both the presence of cutting artefacts, such as tears and folds in the tissue, and the variability in image intensity.

This paper describes the development of an image processing method for assessment of the percentage of epithelium in tissue sections of ovarian tumors, and presents preliminary results obtained with 19 specimens.

## MATERIALS AND METHODS
### Patient Material

Nineteen ovarian tumors were used in this study, including serous, mucinous, and endometrioid types of varying histological grades. Based on standard histopathological criteria, five were diagnosed by a pathologist as borderline (BO), four as well-differentiated carcinomas (WDC), and ten as moderately-poorly differentiated carcinomas (MPDC).

Standard tissue fixation (10% neutral formalin, for approximately 24 h at room temperature), dehydration in alcohol of increasing strength, and embedding in paraplast were performed. With this protocol a majority of quantitative image features remain stable (20). Standard sections, 4-$\mu$m thick, were prepared and stained with Haematoxylin-Eosin for visual inspection.

To discriminate epithelium from stroma, a stoichiometric stain or a component-specific stain is preferable to facilitate the image segmentation. An extensive comparison was performed of various staining techniques (18), such as the Feulgen stains [pararosanilin, thionin (7), and acriflavin (14,19)], Sirius red, and keratin. The evaluation of these stains for applicability in image processing was based on spectral specificity and component specificity. Among all collagen-specific staining methods, Sirius red is found to be the best one. However, this stain is not yet specific enough for all specimens of this study.

The keratin stain, which is epithelium-specific, should suit well, but special fixation and tissue processing are required to obtain reliable results. For this reason, the keratin stain has been set aside for the moment.

In the standard Feulgen procedure, sections were hydrolyzed in 5N HCl for 30 minutes and stained with a solution of 0.5 g pararosanilin in a mixture of 15 ml 1N HCl and a solution of 0.5 g K2S205 in 85 ml distilled water for 45 minutes. The sections then were stained for 5 seconds with a solution of 0.1 g naphthol yellow in a mixture of 100 ml distilled water and 1 ml concentrated acetic acid. This procedure gives good spectral separation of the dyes and has been selected for the present study.

### Image Acquisition

The selected staining method colors the nuclei reddish-brown and the other tissue components yellow. A monochromatic blue filter ($\lambda$ = 420 nm; $\Delta\lambda$ < 10 nm, Schott, Tiel, The Netherlands) for which naphthol yellow shows maximum absorption, is used to distinguish the total area of tissue (both nuclei and cytoplasm) from the background area. A monochromatic yellow filter ($\lambda$ = 552 nm; $\Delta\lambda$ < 10 nm) for which the Feulgen pararosanilin shows maximum absorption, is used to distinguish the nuclei of both epithelium and stroma from the cytoplasm and the background area.

One image pair was recorded per field using the two filters sequentially on a Zeiss UEM microscope (Carl Zeiss, Oberkochen, Germany) fitted with a Vidicon TV-camera (Bosch, Germany). The choice of the optical magnification has been a subject of study, as it could facilitate the image segmentation. With a high optical magnification, a considerable number of images has to be investigated to arrive at a reliable estimate. Another consequence of a high optical magnification is that a greater portion of the tissue lies in the edge regions of the digital image. A low optical magnification will minimize edge-effects, but may cause an unacceptable loss of image detail and accuracy. Consequently, a 6.3× objective with a N.A. of 0.16 (Carl Zeiss, Oberkochen, Germany) was used, which corresponded to a 182× overall magnification at camera level. This magnification resulted in a pixel-to-pixel distance of 1.78 $\mu$m at the specimen level.

Six images per slide were selected from the most epithelium-rich areas of the specimen. For the malignant specimens the total of six could not be acquired, so the number of images was restricted to four.

The images were analyzed on a Kontron Image Processing System (Kontron Bildanalyse GmbH, Eching, Germany). The total dataset consisted of 78 image pairs, each image of which measures 512 × 512 pixels, digitized to 8 bits per pixel.

Table 1
*Percentage of Epithelium From Interactive Morphometry (Control), and Estimated Epithelial Percentage per Specimen From Digital Image Processing*

| Specimen[a] | Percentage of epithelium | |
|---|---|---|
| | Control | Image processing |
| **BO** | | |
| OV01 | 23.5 | 19.9 |
| OV02 | 11.8 | 17.9 |
| OV03 | 22.7 | 29.8 |
| OV04 | 9.1 | 10.3 |
| OV05 | 47.2 | 51.7 |
| **WDC** | | |
| OV06 | 54.1 | 53.7 |
| OV07 | 34.1 | 36.4 |
| OV08 | 35.8 | 30.4 |
| OV09 | 55.6 | 51.5 |
| **MPDC** | | |
| OV10 | 80.2 | 76.3 |
| OV11 | 80.7 | 77.8 |
| OV12 | 73.8 | 63.3 |
| OV13 | 72.3 | 68.6 |
| OV14 | 79.0 | 67.1 |
| OV15 | 75.9 | 85.2 |
| OV16 | 79.6 | 76.2 |
| OV17 | 70.8 | 70.9 |
| OV18 | 84.0 | 72.6 |
| OV19 | 77.0 | 77.3 |

[a]BO, borderline; WDC, well-differentiated carcinoma; MPDC, moderately to poorly differentiated carcinoma.

To correct the images for shading, an image pair was recorded from an empty microscopic field. From these recordings a pair of shading images was defined by smoothing them. The smoothing consisted of three steps: a rank filter (80th centile) followed by an averaging filter and a median filter (50th centile; windowsize 15 × 15 pixels). The rank filter was used to reduce the variance. In particular, oscillations in intensity with a period less than the window width are smoothed, while contours of regions larger than the window used are preserved, without blurring the image (11). The median filter was used with the averaging filter and the rank filter to smooth out slightly ragged contours left by the rank filter (13).

## Interactive Morphometry

To facilitate evaluation and gauging of the image processing results, the control percentages of the epithelial and stromal areas of each specimen were measured via interactive morphometry. The morphometry was performed on all fields selected for digitization. For assessment of the control percentage of epithelium, a 168-point regular grid (21) was used. This grid was randomly positioned on the image and data points overlying epithelium, stroma (together forming the tissue) and lumen (outside the tissue) were accumulated separately.

The number of points on tissue varied from 400 to 700 per specimen, where the points overlying the lumen were ignored. As shown in Table 1, the percentage of epithelium in the borderline and malignant specimens ranged from 10 to 84%. The control percentage was measured for each image a second time after repositioning the grid on the image randomly. The correlation between the first and second assessment of the epithelial percentages of all specimens was 0.996. Therefore it can be concluded that these interactive measurements provide a good reference for image processing results.

## Processing the Blue Image

The image processing method for the assessment of the desired epithelium: tissue ratio consists of two parts. One part concerns the processing of the blue image to determine the area of tissue (epithelium and stroma). The second part concerns the processing of the yellow image to determine the epithelial area. For the determination of the area of tissue, first the blue image was automatically segmented. The image processing for this image consisted of the following steps (Fig. 1):

1. Shading correction: the image was corrected for shading, subtracting the aforementioned blue shading image.

2. Segmentation of tissue: the image was segmented at a global threshold. If the smoothed grey level histogram had only one peak, it was assumed that the image contained tissue only. This is a valid assumption for all blue images in the dataset, which had a unimodal grey level distribution. If the smoothed histogram had two peaks, the image contained both tissue and lumina. To minimize the probability of misclassifying an object

point as background point or vice versa (9, 22), the minimum between the two peaks has been selected as threshold level (Fig. 2). For our purposes, this threshold selection method results in an acceptable threshold level.

3a. Elimination of small objects: remaining difficulties are small artefacts in the background area and tears or holes in the tissue. Small objects in the thresholded binary image were eliminated and small tears or holes were repaired.

First, minimal tissue holes were repaired using a closing operation (4-connected) with a stepsize of 1 pixel. This operation, a dilation followed by an erosion, effectively filled holes with a cross-size smaller than approximately 3.6 μm, the size chosen in order to preserve small isolated nuclei.

Small objects in the background were then eliminated by application of a tenfold erosion operation (4-connected), which removed objects with a cross-size smaller than 35 μm. The cross-size used had been set to such a value that small objects (such as loose single cells, dirt, or staining material) were eliminated, the intent being to preserve small epithelial areas surrounding stroma.

3b. Repairing small tissue holes: small tears or holes in the tissue were repaired if the smallest dimension was less than 17.8 μm through application of a fivefold erosion operation, 4- and 8-connected. Closing holes or
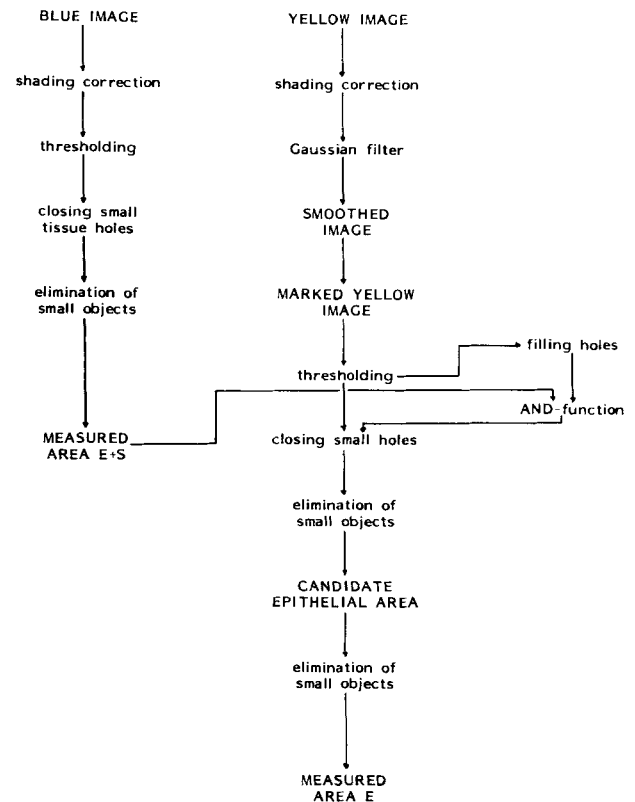


FIG. 1. Scheme of the image processing steps for the blue and the yellow images to estimate respectively the total area of tissue and the area of epithelium.
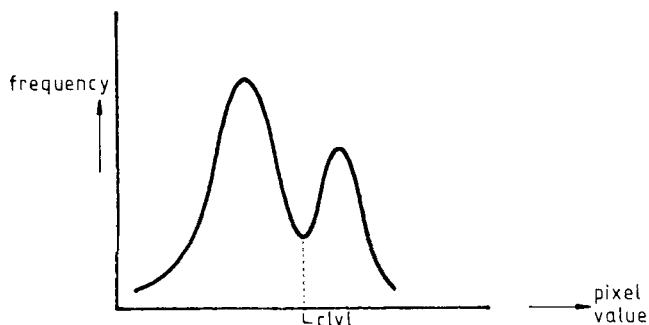
FIG. 2. Example of a smoothed grey level histogram of the blue image. The distribution is bimodal. The minimum between the two peaks is selected as the threshold (CLVL).
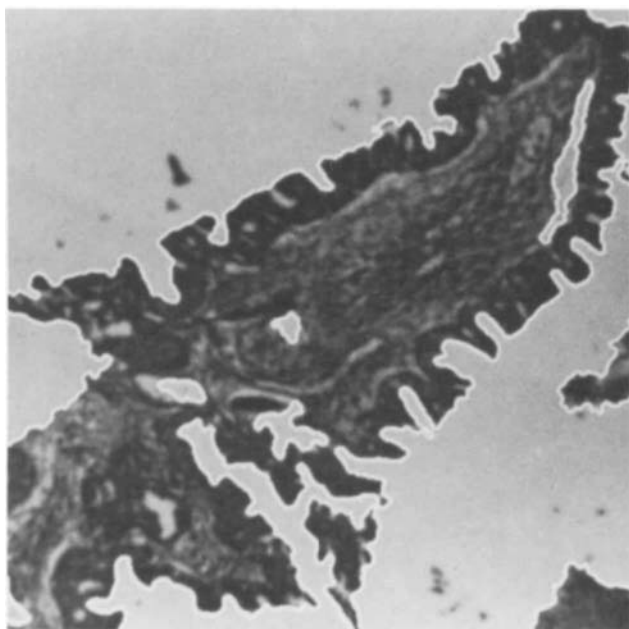


FIG. 3. Example of a blue image, coming from a borderline ovarian tumor. The white, 2-pixel-thick lines give the contours of the estimated area of tissue.

tears in the tissue with a larger cross-size would enclose small lumen areas, while using a smaller cross-size would remove small tissue areas.

This resulted in the estimated area of tissue (see an example of a borderline ovarian tumor in Fig. 3). In this figure the overlayed contours represent the estimated area of tissue.

## Processing the Yellow Image

Subsequently, the yellow image was also segmented automatically to determine the area of epithelium. The image processing for the yellow image is based on the observation that, in general, epithelial nuclei are more tightly packed than stromal nuclei. For that reason, a structural approach was applied to discriminate epithe-

lium from stroma. The processing of the yellow image consisted of the following steps (Fig. 1):

1. Shading correction: the image was also corrected for shading by subtraction of the aforementioned yellow shading image.

2. Gaussian blurring: seeing that epithelial nuclei are more tightly packed than stromal nuclei, segmentation of the epithelial area could be facilitated by bridging the epithelial nuclei before thresholding the yellow image. A 3 × 3 linear Gaussian filter, of which the coefficients follow a two-dimensional Gaussian distribution with a standard deviation of 0.85, was used to smooth the density mass of the nuclei.

3. Segmentation of nuclei: in the yellow images the grey value distribution is unimodal. This distribution can vary strongly for the different pathological types, due to a strong variety of intensity values of both epithelial and stromal nuclei. As the threshold selection algorithm should be resistant against variability in staining intensity, the threshold selection is based on the image contrast range (i.e., the difference between the minimum pixel value in the histogram and the lumen peak-value). Due to the fact that naphthol yellow shows some absorption at 552 nm, the peak in the histogram can result from either cytoplasm absorption or lumen absorption or a combination of the two. Therefore it was not possible to properly determine the lumen peak value from this histogram alone. To overcome this problem, the peak was split into two, one associated with lumen and the second one associated with cytoplasm.

For the computation of the lumen peak (mod l) a histogram was formed from the lumen pixels, by use of the segmented blue image, computed previously, as a mask (Fig. 4a).

For the cytoplasm peak value, a histogram was formed from the tissue pixels resulting from the blue image segmentation, and the mode was calculated (mod c). This histogram also provided the absorption minimum intensity (min) in the yellow image, skipping the 0.5% extreme minimum values (Fig. 4b).

From the image contrast range in the density domain, i.e., $\log(\text{min}) - \log(\text{mod } l)$, the threshold level (lvl) was computed from:

$$\log(\text{lvl}/\text{mod } c) = C \times \log(\text{min}/\text{mod } l).$$

The parameter C can be tuned such that priority is given to detect most or all epithelial nuclei, to get a good segmentation result for the moderately to poorly differentiated carcinomas. For all specimens, C was fixed at C = 0.168.

4a. Filling epithelial cytoplasm: given this primary segmentation (Fig. 5a,b), for the determination of the epithelial area, small objects in the binary image must be removed and small spaces between the epithelial nuclei filled, bridging the epithelial nuclei. To prevent the elimination of single epithelial nuclei, first all holes in the binary image were filled before small objects were eliminated.
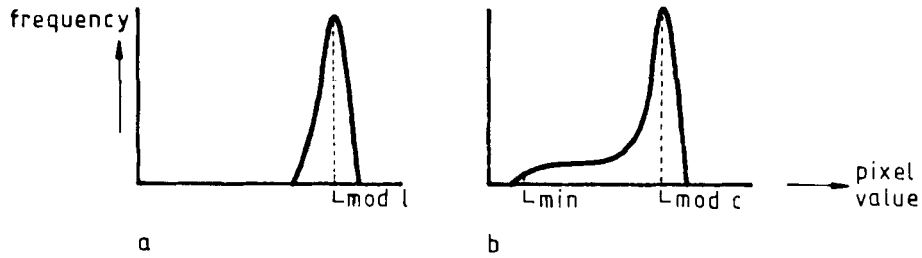
FIG. 4. a) Example of a histogram formed from the lumen pixels, using the segmentation result of the blue image as a mask in the yellow image, to compute the lumen peak (mod l). b) Example of a histogram formed from the tissue pixels to calculate the cytoplasm peak value (mod c) and the minimum intensity (min).
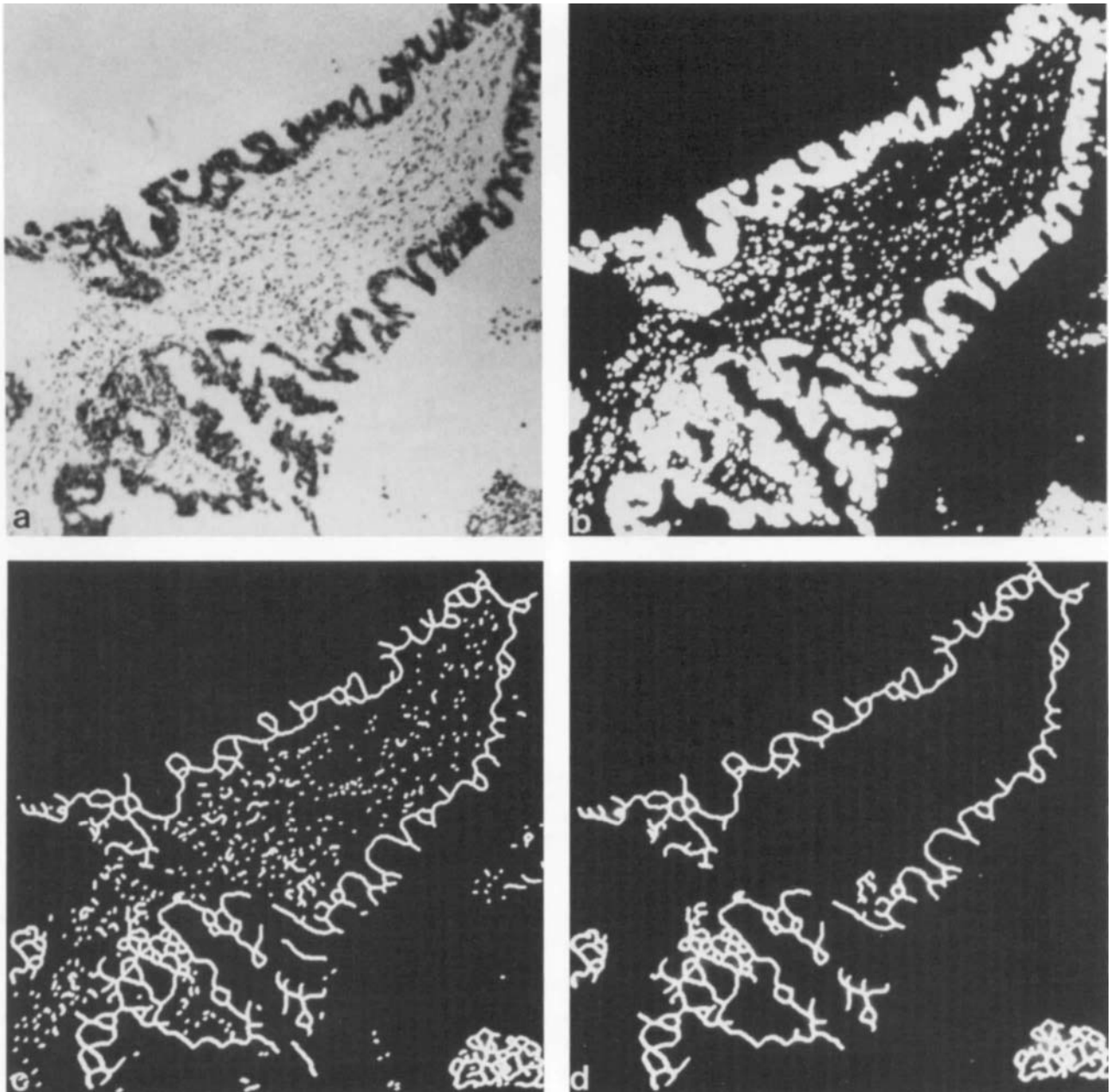


FIG. 5. a) The yellow image after shading correction. b) The thresholded binary image. c) Result of the closing operation and the skeleton operation before the elimination of stromal nuclei. d) Result after removing small skeleton parts, coming from stromal nuclei.
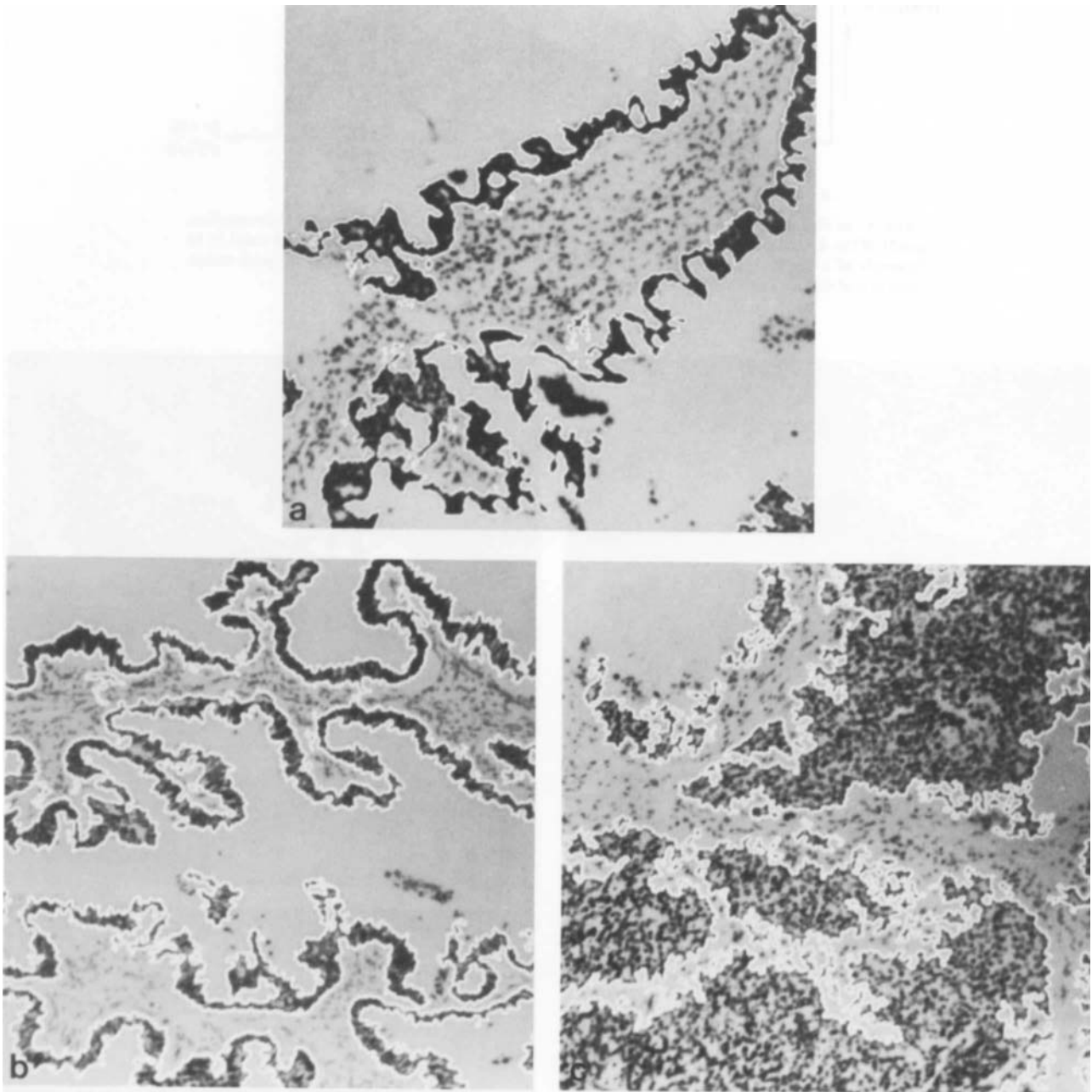
FIG. 6. Examples of yellow images, from which the area of epithelium is estimated. The white, 2-pixel-thick lines give the contours of the estimated areas of epithelium. a) Image from a borderline ovarian tumor. b) Image from a well-differentiated ovarian tumor. c) Image from a moderately to poorly differentiated ovarian tumor.

4b. Elimination of stromal nuclei: for the elimination of small objects, mostly stromal nuclei, the skeleton operation was first applied, to maintain connection between the epithelial pixels. This operation was followed by a closing (4-connected) with a stepsize of 2 pixels, to fit small epithelial gaps (Fig. 5c). Then the skeleton parts not exceeding 50 pixels were removed (Fig. 5d). The result is the so-called candidate epithelial area.

4c. Closing small holes in the candidate epithelial area: application of a twofold skeleton operation followed by a twofold erosion operation (4- and 8-connected) closed holes in the candidate epithelial area with a cross-size smaller than 14 $\mu$m. Filling holes with a larger diameter also closed holes and tears in the stromal area, and a smaller cross-size would result in an "under-estimation" of the epithelial area.

D.I.P. OVARIAN TUMOURS
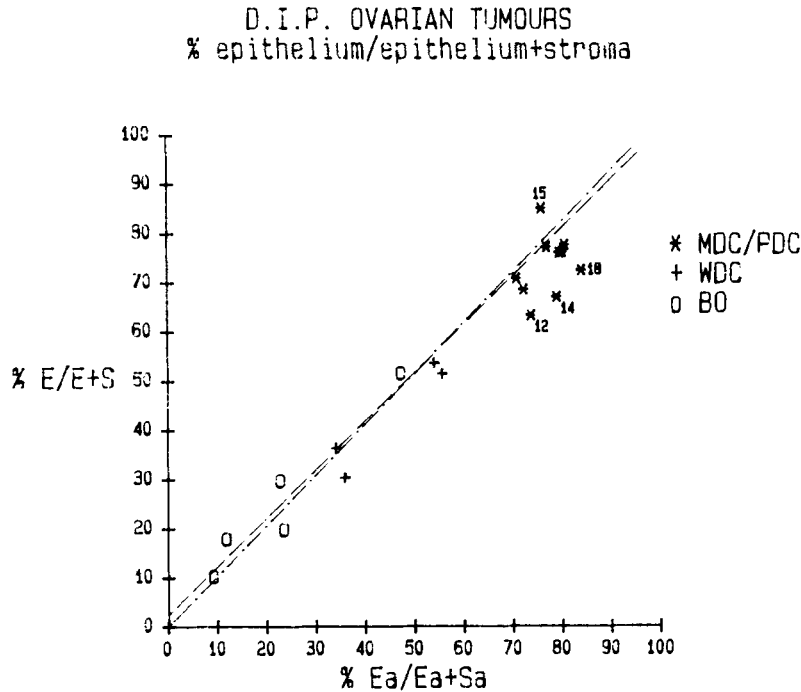% epithelium/epithelium+stroma



FIG. 7. Results of the image analysis, % E/E + S, related to the control percentages, % Ea/Ea + Sa. The correlation coefficient r is 0.98 and the slope of the best linear fit is 0.92. E, number of pixels in the epithelial part, measured by digital image processing; S, number of pixels in the stromal part, measured by digital image processing; Ea, number of points overlying the epithelial part, established morphometrically; Sa, number of points overlying the stromal part, established morphometrically. MDC/PDC, moderately or poorly differentiated; WDC, well-differentiated; BO, borderline.

The result of this procedure is the area of epithelium, estimated from the yellow image. Figure 6a, b, c shows the contours of the estimated areas of epithelium for a borderline, a well-differentiated, and a moderately to poorly differentiated ovarian carcinoma.

### RESULTS

Examples of the results are shown in Figure 7. Notice that for three moderately to poorly differentiated specimens (OV12, OV14, and OV18) the estimated epithelial area is smaller than the measured control percentage. This is due to the observed fact that for these specimens the epithelial nuclei are less closely packed, which results in an underestimation of the epithelial percentage. For these specimens the maximum difference is approximately 10% at slide level and hence neglectable. For the poorly differentiated specimen OV15, image analysis results in an estimated epithelial percentage greater than the interactive approach. This was caused by areas of tightly packed stromal nuclei and the presence of dark, tightly packed lymphocytes in the stromal areas.

The epithelial percentages are displayed in Table 1. It can be seen from this table that the detected area of epithelium increases with increasing histological grade. For the cases under study, the borderline tumors and well differentiated carcinomas have an estimated area percentage smaller than 55%. The measured percentages vary from 63 to 85% for the moderately to poorly

differentiated carcinomas. Comparison of the image processing results with the area percentages resulting from interactive morphometry (Fig. 7) shows a strong correlation (r = 0.98). The slope of the best linear fit is 0.92.

### DISCUSSION

The objective of this study is to investigate the possibility of automatically estimating the volume percentage of epithelium in (tumor) tissue.

In previous studies (2,4), the epithelial volume has been estimated through interactive morphometry by positioning a counting grid on the epithelium-rich microscopic fields of the specimen. Practical application in diagnostic pathology, however, requires accurate counting of points, overlying the epithelial and stromal parts. To reach sufficient accuracy, a considerable number of microscopic tissue fields is required. For that reason, the point-counting method is a tedious and time-consuming task. Digital image processing was explored as a means of estimating the epithelial volume automatically.

For the (ovarian) specimens under study, the image processing method gives good results; comparison with the control percentages resulting from interactive morphometry shows a strong correlation (r = 0.98). The measured percentages vary from 10 to 55% for borderline and well-differentiated carcinomas and from 63 to 85% for moderately to poorly differentiated carcinomas, showing the increase with histological grade.

The dataset at the moment is relatively small. To correlate the image processing results to the prognosis of patients, more patient material is being investigated.

Given the reliability of the results, it can be concluded that the automated method also offers practical advantages over the interactive morphometrical assessment. The image processing method takes 6 minutes, whereas the point-counting method takes 20 minutes per specimen. To overcome the problem of misestimation, caused by the epithelial nuclei being less closely packed or the presence of tightly packed lymphocytes in the stromal areas, an epithelium-specific stain could be used. Such an epithelium-specific stain, for example the keratin stain suitable for paraffin embedded tissue (17), provides a direct estimate of the epithelial volume. A limitation of the keratin stain, however, is that the number of keratin filaments in epithelial cells of moderately to poorly differentiated carcinomas can be decreased, compared to well-differentiated carcinomas. This keratin staining procedure is presently being tested for applicability in image processing of paraffin embedded tissue.

In this study, the image processing method has been tested on ovarian specimens, but is expected to be applicable to tumors of other organs as well. Potential candidates are endometrial tumors and prostatic cancers (6). In breast cancers and malignant melanomas, quantitative microscopic features were shown to be prognostically important in the epithelium-rich, most cellular areas. The image processing method can be of help in selecting these fields objectively.

## ACKNOWLEDGMENTS

## LITERATURE CITED

1. Atkin NB, Kay R: Prognostic significance of modal DNA value and other factors in malignant tumours, based on 1465 cases. Br J Cancer 40:210–217, 1979.
2. Baak JPA, Agrafojo Blanco A, Kurver PHJ, Langley FA, Boon ME, Lindeman J, Overdiep SH, Nieuwlaat A, Brekelmans E: Quantitation of borderline and malignant mucinous ovarian tumours. Histopathology 5:353–360, 1981.
3. Baak JPA, Lindeman J, Overdiep SH, Langley FA: Disagreement of histopathological diagnoses of different pathologists in ovarian tumors—with some theoretical considerations. Eur J Obstet Gynecol Reprod Biol 13:51–55, 1982.
4. Baak JPA, Wisse-Brekelmans ECM, Langley FA, Talerman A,

Delemarre JFM: Morphometric data to FIGO stage and histological type and grade for prognosis of ovarian tumours. J Clin Pathol 39:1340–1346, 1986.
5. Breitenecker G, Bartl W, Scheiber V: Die Prognostischen bedeutung morphologischer Parameter bei malignen epithelialen Ovarialtumoren. Pathologe 4:29–40, 1983.
6. Cantrell BB, Klerk DP de, Eggleston JC, Boitnott JK, Walsh PC: Pathological factors that influence prognosis in stage A prostatic cancer: The influence of extent versus grade. J Urol 125:516–520, 1981.
7. Duijn P van: A histochemical specific Thionin-SO2 reagent and its use in a bi-color method for deoxyribonucleic acid and periodic acid schiff positive substances. J Histochem Cytochem 4:55–63, 1956.
8. Friedlander ML, Hedley DW, Taylor IW, Russell P, Coates AS, Tattersall MHN: Influence of cellular DNA content on survival in advanced ovarian cancer. Cancer Res 44:397–400, 1984.
9. Fu KS, Mui JK: A survey on image segmentation. Pattern Recognition 13:3–16, 1981.
10. Hernandez E, Bhagavan BS, Parmley TH, Rosenshein NB: Interobserver variability in the interpretation of epithelial ovarian cancer. Gynecol Oncol 17:117–123, 1984.
11. Hodgson RM, Bailey DG, Naylor MJ, Ng ALM, McNeill SJ: Properties, implementations and applications of rank filters. Image and Vision Computing 3:3–14, 1985.
12. Kaman EJ, Smeulders AWM, Verbeek PW, Young IT, Baak JPA: Image processing for mitoses in sections of breast cancer: A feasibility study. Cytometry 5:244–249, 1984.
13. Lester JM, Brenner JF, Selles WD: Local transforms for biomedical image analysis. Comput Graph Im Proc 13:17–30, 1980.
14. Levinson JW, Retzel S, Mccormick JJ: An improved Acriflavin Feulgen method. J Histochem Cytochem 25:355–358, 1977.
15. Malkasian GD, Melton III LJ, O'Brien PC, Greene MH: Prognostic significance of histologic classification and grading of epithelial malignancies of the ovary. Am J Obstet Gynecol 149:274–284, 1984.
16. Morrow CP: Malignant and borderline epithelial tumors of ovary: Clinical features, staging, diagnosis, intraoperative assessment and review of management. In: Gynecological Oncology, Coppleson M (ed). Vol. 2: Churchill Livingstone, New York, 1982, pp 655–680.
17. Ramaekers FCS: Application of antibodies to intermediate filament proteins as tissue specific probes in the flow cytometric analysis of complex tumors. Presented at the International Conference Analytical Cytology XI, South Carolina, 1985.
18. Schipper NW, Smeulders AWM, Baak JPA: Comparison of different cell or tissue component specific stains, suited for image processing. In preparation.
19. Tanke HJ, van Ingen EM, Ploem JS: Acriflavine-Feulgen Stilbene staining: A procedure for automated cervical cytology with a television based system (LEYTAS). J Histochem Cytochem 27:84–86, 1979.
20. Thunnissen FBJM, Baak JPA, Diegenbach PC: Fixation induced variations in quantitative nuclear image features in sections. Acta Histochem 68:218–226, 1981.
21. Weibel ER: Sterelogical principles for morphometry in electron microscopy. Int Rev Cytol 26:235–302, 1969.
22. Weszka JS: A survey of threshold selection techniques. Comput Graph Im Proc 7:259–265, 1978.